Trace element, rare earth element and trace carbon compounds in Subglacial Lake Whillans, West Antarctica

Turetta, Clara; Barbaro, Elena; Skidmore, Mark L.; Gambaro, Andrea; Michaud, Alexander B.; Mitchell, Andrew C.; Vick-Majors, Trista J.; Priscu, John C.; Barbante, Carlo

Published in:
Science of the Total Environment

DOI:
10.1016/j.scitotenv.2023.164480

Publication date:
2023

Citation for published version (APA):
Turetta, C., Barbaro, E., Skidmore, M. L., Gambaro, A., Michaud, A. B., Mitchell, A. C., Vick-Majors, T. J., Priscu, J. C., & Barbante, C. (2023). Trace element, rare earth element and trace carbon compounds in Subglacial Lake Whillans, West Antarctica. *Science of the Total Environment*, *892*, Article 164480. https://doi.org/10.1016/j.scitotenv.2023.164480

Science of the Total Environment 892 (2023) 164480

Contents lists available at ScienceDirect

Science of the Total Environment

journal homepage: www.elsevier.com/locate/scitotenv

Trace element, rare earth element and trace carbon compounds in Subglacial Lake Whillans, West Antarctica

Clara Turetta [a,b], Elena Barbaro [a,b,*], Mark L. Skidmore [c], Andrea Gambaro [a,b], Alexander B. Michaud [d], Andrew C. Mitchell [e], Trista J. Vick-Majors [f], John C. Priscu [g], Carlo Barbante [a,b]

[a] Institute of Polar Sciences CNR, Via Torino 155, 30172 Mestre-Venezia, Italy
[b] Department of Environmental Sciences, Informatics and Statistics, University of Venice, Ca' Foscari, Via Torino 155, 30172 Mestre-Venezia, Italy
[c] Department of Earth Sciences, Montana State University, Bozeman, MT 59717, USA
[d] Bigelow Laboratory for Ocean Sciences, East Boothbay, ME 04544, USA
[e] Department of Geography and Earth Sciences, Aberystwyth University, Aberystwyth, Wales, UK
[f] Department of Biological Sciences and Great Lakes Research Center, Michigan Technological University, Houghton, MI, USA
[g] Polar Oceans Research Group, Sheridan, MT 59749, USA

HIGHLIGHTS

- Lake water and porewaters from Subglacial Lake Whillans (Antarctica) were analysed
- Hydrological features highlighted using rare earth elements and organic compounds
- Redox changes in subglacial lake porewater
- Free amino acids highlight tight cycling of N-rich compounds
- Vanillic acid-to-vanillin ratio suggests an oxidative degradation

GRAPHICAL ABSTRACT

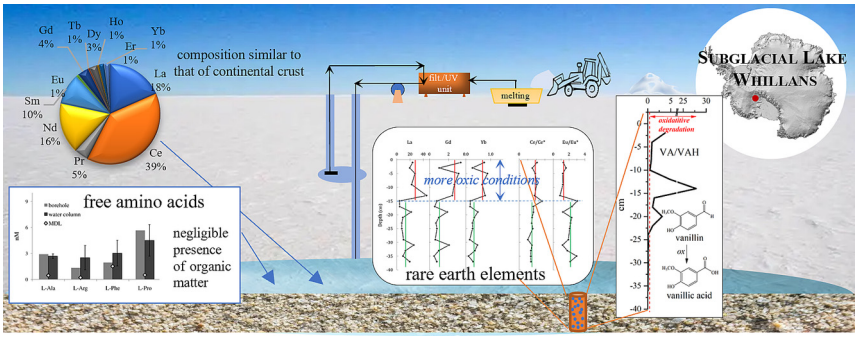

ARTICLE INFO

Editor: Damia Barcelo

Keywords:
Lake water
Porewater
Redox conditions
West Antarctica
SLW
REE
TE
Amino acids
Phenolic compounds

ABSTRACT

Whillans Subglacial Lake (SLW) lies beneath 801 m of ice in the lower portion of the Whillans Ice Stream (WIS) in West Antarctica and is part of an extensive and active subglacial drainage network. Here, the geochemical characterization of SLW rare earth elements (REE), trace elements (TE), free amino acids (FAA), and phenolic compounds (PC) measured in lakewater and sediment porewater are reported. The results show, on average, higher values of REEs in the lakewater than in the porewater, and clear changes in all REE concentrations and select redox sensitive trace element concentrations in porewaters at a depth of ~15 cm in the 38 cm lake sediment core. This is consistent with prior results on the lake sediment redox conditions based on gas chemistry and microbiological data. Low concentrations of vanillyl phenols were measured in the SLW water column with higher concentrations in porewater samples and their concentration profiles in the sediments may also reflect changing redox conditions in the sediments. Vanillin concentrations increased with depth in the sediments as oxygenation decreases, while the concentrations of vanillic acid, the more oxidized component, were higher in the more oxygenated surface sediments. Collectively these results indicate redox changes occurring with the upper 38 cm of sediment in SLW and provide support for the existence of a seawater source, already hypothesized, in the sediments below the lowest measured depth, and of a complex and dynamic geochemical system beneath the West Antarctic Ice Sheet.
Our results are the first to detail geochemical properties from an Antarctic subglacial environment using direct sampling technology. Due to their isolation from the wider environment, subglacial lakes represent one of our planets

* Corresponding author at: Via Torino 155, 30172 Mestre-Venezia, Italy.
E-mail address: elena.barbaro@cnr.it (E. Barbaro).

http://dx.doi.org/10.1016/j.scitotenv.2023.164480
Received 17 February 2023; Received in revised form 8 May 2023; Accepted 24 May 2023
Available online 30 May 2023

last pristine environments that provide habitats for microbial life and natural biogeochemical cycles but also impact the basal hydrology and can cause ice flow variations.

1. Introduction

Lakes beneath the Antarctic Ice sheet were initially discovered during the 1970s (Robin et al., 1970). Based on radar data and satellite measurements we now know that >650 subglacial lakes exist beneath the East and West Antarctic Ice Sheets (Gudlaugsson et al., 2016; Wright and Siegert, 2012; Livingstone et al., 2022). Antarctic subglacial lakes are frequently located either in the ice-sheet interior, close to ice divides where the surface slopes are low and the ice is thick, or in areas of higher ice velocity, where internal ice deformation, sliding and geothermal heating are sufficient to produce melting at the base (Dowdeswell and Siegert, 1999; Siegert, 2000; Priscu et al., 2008; Gudlaugsson et al., 2016; Siegert et al., 1996; Christner et al., 2014; Priscu et al., 2021; Livingstone et al., 2022). Basal water then flows under gravity and overburden ice pressure where it collects in geomorphic basins. Subglacial lakes range from major subglacial troughs that are several tens of kilometers long, to small, 1-km long lakes located in broad flat regions or subglacial highlands (Dowdeswell and Siegert, 1999). Geophysical and remote sensing investigations have demonstrated that many subglacial lakes are "active", being part of connected subglacial drainage systems characterized by periodic fill and drain events on monthly to decadal scales (Ashmore and Bingham, 2014; Smith et al., 2009; Wright and Siegert, 2012; Siegfried et al., 2023; Venturelli et al., 2023). The subglacial hydrological system has a key influence on the geochemical and biological composition of subglacial environments, including lakes; thus these periodic discharges (Fricker et al., 2011; Wingham et al., 2006) impact lake biogeochemical properties (Michaud et al., 2016; Vick-Majors et al., 2016), and then fertilize coastal marine environments (Vick-Majors et al., 2020a). Our study represents geochemical data from the first subglacial lake, Whillans Subglacial Lake (SLW) directly sampled using clean drilling technology. Here is presented a comprehensive analysis of the trace element and organic composition of lake and porewaters, due to their importance toward understanding biogeochemical processes occurring in subglacial lakes, and potential inputs to downstream coastal marine systems (e.g. Carter and Fricker, 2012; Vick-Majors et al., 2020a).

To date, select trace inorganic and organic compounds have not been determined in subglacial lakes which may offer utility in understanding fine scale redox changes, the relationship to microbial activity and the sources of organic carbon. Rare earth elements (REE) and select trace elements (TE) are sensitive redox indicators (e.g. Elderfield et al., 1990; Byrne and Sholkovitz, 1996) and can be used to evaluate observed redox changes in sediments. Similarly, free amino acids (FAA) can be released from living cells and by cellular lysis in aquatic ecosystems (Bronk et al., 1994). The occurrence of amino acids within the water column and sediments may therefore be a measure of microbial activity which in turn is influenced by oxygen availability (Achberger et al., 2016; Christner et al., 2014; Vick-Majors et al., 2016; Vick-Majors et al., 2020a). Conversely, terrestrial carbon inputs (Edelkraut, 1996) can be determined by Phenolic compounds (PC) that are the products of biomass burning (e.g. Saltzman et al., 2014) or the degradation of lignin.

Here we present the first measurements of REE, TE, FAA and PC from the water column and sediment porewater of an Antarctic subglacial lake (SLW) to determine fine scale redox changes and the type and sources of organic matter in the water column and sediment porewater.

2. Background and analytical protocols

2.1. Study site

SLW is located beneath 800 m of ice of the Whillans Ice Stream and approximately 70 km upstream of the grounding line where the Whillans Ice Stream (WIS) begins to float over the Ross Sea (Carter et al., 2013; Fricker and Scambos, 2009; Fricker et al., 2007) (Fig. 1). SLW is a shallow lake with a depth of ~2.2 m in 2013, the time of sampling, (Christner et al., 2014), and is part of an extensive and evolving subglacial drainage network that resembles a large wetland running along the Siple Coast of West Antarctica (Fisher et al., 2015; Fricker et al., 2007; Siegfried et al., 2016; Siegfried et al., 2014; Priscu et al., 2021). The subglacial lakes in this region, e.g. SLW, SLM –Mercer Subglacial Lake, SLC - Conway Subglacial Lake (Fig. 1) are "active" subglacial lakes that drain and refill on sub-decadal time scales discharging water toward the Ross Sea (Siegfried et al., 2016; Siegfried et al., 2014).

The primary source of water to SLW is ice melt (Christner et al., 2014) and the SLW water column and sediment porewaters are a sodium-chloride type, typical of marine and deep, ancient ground waters, where mineral weathering is also a solute source (Michaud et al., 2016; Gustafson et al., 2022). A marine source for a portion of the solute in SLW is supported by a Br^-:Cl^- ratio close to marine values in the SLW water column (Christner et al., 2014). SLW water column samples had a high proportion of very fine particulate and colloidal material. Complete settling of the suspended material in the SLW water column sample did not occur even after more than three years storage at 4 °C (Fig. S1). Sediment on the lake floor consists of till, which is unsorted and lacking in structure, which was deposited when the ice sheet was grounded, and there was no evidence for erosion or deposition by flowing water on the lake floor (Hodson et al., 2016). The till at SLW had a high proportion (50 %) of silt/clay size particles and showed a composition similar to tills found upstream of SLW (Michaud et al., 2016). There is an active microbial community in the lake waters and sediments (Christner et al., 2014; Achberger et al., 2016; Vick-Majors et al., 2016) and multiple lines of evidence, including methane concentration, methane isotopic composition and methanotrophic gene abundance indicate a marked change in the redox conditions in the lake sediments at a depth of ~15 cm, with limited evidence for oxygen below that depth (Michaud et al., 2016).

2.2. Sample collection and processing

A clean hot-water drill was used to reach SLW; the drilling system created a borehole through about 800 m of ice overlying the SLW. In order to ensure that borehole water and SLW samples (water and sediment) maintain their integrity, a borehole water treatment system, designed to remove particulates >0.2 μm in diameter and reduce the concentration of viable microbial cells present in the borehole water, was used (Priscu et al., 2013; Michaud et al., 2020). Lake water from three discrete hydrocasts collected samples from mid-depth in the water cavity. A borehole water sample, which was snow and ice melt circulated through the hot water drill (Rack et al., 2014), was collected 700 m below the ice surface (~100 m above the water cavity) before lake breakthrough as a control to confirm that drill-water was not introduced to the lake (Priscu et al., 2013; Michaud et al., 2020). Lake and borehole water were collected with a clean 10 L Niskin bottle and decanted into 30 mL pre-cleaned LDPE bottles. Logistical constraints did not allow us to take an anaerobic chamber into the field; to prevent oxidation processes take place we tried to minimize contact between the samples and air by capping with a meniscus and kept the samples cold and dark and then frozen until the analysis. The 30 mL bottles were rinsed with ultrapure nitric acid (Romil LTD – UPA-grade) and ultrapure water (ELGA-Vivendi Water Systems, Bucks, UK) under a Class-100 laminar flow bench-hood, inside a Class-1000 clean room at ISP-CNR (former IDPA-CNR), Ca' Foscari University of Venice (Turetta et al., 2004). SLW water samples were processed inside a Class-1000 clean room at ISP-CNR, Ca' Foscari University of Venice and prepared as follows: one aliquot (1.5 mL) of filtered (F) water (single-use syringe filter with PTFE membrane 0.20 μm, Sartorius Stedim Biotech GmbH, Goettingen, Germany) and one aliquot (1.5 mL) of unfiltered (NF) water were diluted 10-

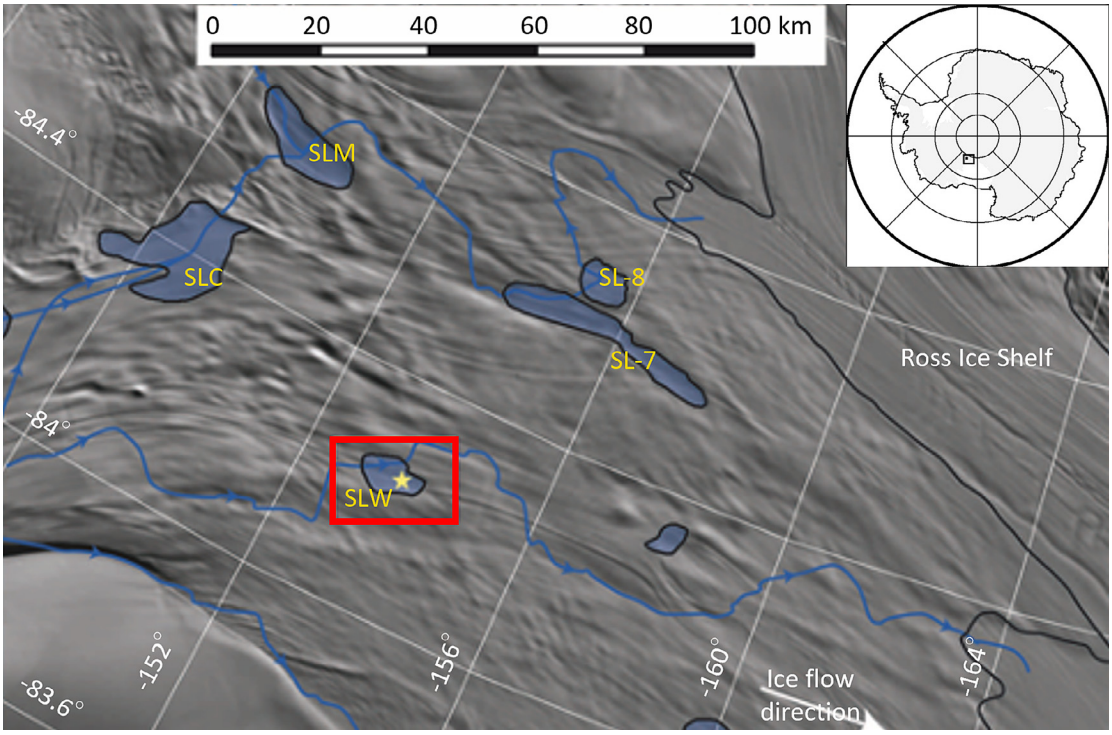

Fig. 1. Map showing SLW (red rectangle) and other subglacial lake locations. The yellow star indicates the approximate location of drilling site (84.240°S, 153.694°W). Blue line with arrows indicates modelled water flow paths (from Christner et al., 2014, modified). The lake depth at the borehole site was about 2.2 m at the time of sampling.

fold (to prevent the clogging of nebulizer during the analysis) using ultrapure water in pre-cleaned LDPE vials. Filtered and unfiltered aliquots were acidified with ultrapure nitric acid (UPA-grade, 2 % v:v).

Sediment porewater was obtained from a 38 cm long sediment core using a multicoring device (Uwitec) that had a core barrel inner diameter of 59.5 mm and a length of 60 cm. The sediment was composed of a macroscopically structureless diamicton (Tulaczyk et al., 2014; Rosenheim et al., 2023). Eighteen pore water samples were obtained at 2 cm intervals down the 38 cm long core by inserting Rhizon samplers (0.2 μm pore size) into the core through predrilled holes in the core liner and extracting pore fluid under negative pressure into a 10 mL sterile HDPE syringe (Christner et al., 2014; Michaud et al., 2016). Each sample was transferred from the syringe into a pre-cleaned LDPE vial and frozen. The porewater samples were processed at ISP-CNR, Ca' Foscari University of Venice, inside a Class 1000 clean room, under a Class 100 laminar flow hood, and prepared as follows: two aliquots of each filtered sample were diluted 10-fold in pre-cleaned LDPE vials using ultrapure water (ELGA-Vivendi Water Systems, Bucks, UK) to prevent the clogging of nebulizer during the analysis. One diluted subsample was acidified with ultrapure nitric acid (UPA grade, 2 % v:v) and used for inorganic components analysis. The second (unacidifed) aliquot of each diluted pore water sample was used for organic compound analysis.

Borehole and SLW water samples for organic compound analysis were collected directly from the Niskin bottle into 500 mL amber glass bottles that were pre-cleaned with ultrapure water, acetonitrile (Romil LTD - Ultra-grade) and methanol (Romil LTD - Ultra-grade) in a Class 1000 "organic" clean room, under a Class 100 laminar flow hood, at ISP-CNR, Ca' Foscari University of Venice. The preparation of samples and analyses to determine organic compounds were also performed in this Class 1000 clean room. The internal standards, consisting of a standard solution of labeled amino acids (average concentrations about 1 μg L^{-1}) and $^{13}C_6$-vanillin (1 μg L^{-1}), were added to borehole water, SLW water and pore water samples.

2.3. Determination of trace elements (TE) and rare earth elements (REEs)

The analysis to determine inorganic components (TE and REEs) was performed on SLW water and porewater samples 24 h after their preparation and acidification at ISP-CNR, Ca' Foscari University of Venice using an ICP-SFMS (Inductively Coupled Plasma Sector Field Mass Spectrometry - Element2, Thermo Scientific, Bremen, Germany). The instrument was installed in a dedicated laboratory with the sample introduction area protected by a laminar flow cabinet. The sample introduction system was a desolvation unit (Aridus, Cetac Technologies, Omaha, NE, USA) coupled with a PFA μ-flow nebulizer (100 μL min^{-1}): the sample flows in a teflon spray chamber heated up to 95 °C to prevent droplet accumulation, and then is swept by an Ar flow into a semi-permeable membrane (heated up to 165 °C) to significantly reduce the formation of oxides that can interfere with element measurements. Hafnium oxide to hafnium (HfO/Hf), strontium oxide to strontium (SrO/Sr), cerium oxide to cerium (CeO/Ce) and rubidium oxide to rubidium (RbO/Rb), expressed as percentage ratios, were typically monitored to assess the performance of the introduction system. The use of the μ-flow nebulizer coupled with the desolvation unit produced HfO/Hf, SrO/Sr, CeO/Ce and RbO/Rb ratios of 0.0005, 0.06, 0.02 and 0.01 % respectively, showing significantly reduced oxide formation in the plasma (Turetta et al., 2004). The introduction system was connected to the ESI SC2-E2 autosampler (Elemental Scientific, Omaha, NE, USA). The sample introduction system and the autosampler were maintained and operated within a laminar flow hood. Intensity optimisation was carried out daily, using a tuning solution of ultrapure water containing 1 ng/mL of In. Before beginning the analyses, an accurate mass calibration was performed in low-, medium- and high-resolution modes using a solution whose elements had *m/z* values that covered the whole mass range of interest. The quantification of TE and REE was carried out by matched calibration method. The total consumption of sample for REE and TE analysis was ~1.0 mL. Eleven aliquots of lake water sample were spiked for TE with a multi-element standard solution (0, 2, 5, 10, 50, 100, 200, 500, 800,1000, 2500 ng L^{-1}, from a 10 mg L^{-1} ICP-MS calibration standard IMS102-Ultra Scientific (www.ultrasci.com); nine aliquots of lake water sample were spiked for REE with a multi-element standard solution (0, 0.1, 0.2, 0.5, 1, 2, 5, 10, 20, ng L^{-1}, from a 10 mg L^{-1} ICP-MS calibration standard IMS101-Ultra Scientific (www.ultrasci.com). The accuracy of the measurements was determined using a certified reference material (TM-RAIN95) in which the TE concentrations were measured (Supplemental Table 1).

Table 1
REE concentrations in nmol L^{-1} in SLW lake water and borehole samples (CAST-N). Values for SLW filtered water samples are the mean of CAST1 and CAST3 and for unfiltered samples the mean of CAST1, CAST2 and CAST3. Relative standard deviation (RSD) is <5 %, except for Ho, Tm and Lu, where 5 % < RSD < 8 %.

	Filtered (F) acidified		Non-Filtered (NF) acidified	
	CAST-N	Mean of CAST 1 and 3	CAST-N	Mean of CAST 1, 2 and 3
La	0.0288	0.374	0.0274	105.8
Ce	0.0592	0.787	0.0542	224.8
Pr	0.0071	0.091	0.0071	25.5
Nd	0.0340	0.318	0.0305	85.3
Sm	0.0166	0.189	0.0153	49.2
Eu	0.0020	0.018	0.0026	3.0
Gd	0.0057	0.062	0.0051	14.6
Tb	0.0008	0.009	0.0008	1.9
Dy	0.0035	0.045	0.0034	9.8
Ho	0.0008	0.011	0.0010	1.7
Er	0.0021	0.025	0.0020	4.2
Tm	0.0010	0.004	0.0009	2.3
Yb	0.0032	0.024	0.0031	6.4
Lu	0.0006	0.004	0.0006	0.9

2.4. Determination of free amino acids (FAA) and phenolic compounds (PC)

The SLW water samples were placed in an ultrasonic bath for 30 min at room temperature in order to improve the release of the water-soluble material sorbed onto the particulate matter. An aliquot of each sample was then filtered through a 0.2 μm PTFE filter before the determination of PC. Another aliquot for amino acid determination was passed through a strong-anion exchange cartridge, pre-cleaned with methanol and water, to remove the anionic compounds (i.e. sulfate and bisulfate) that cause matrix effects during the HPLC-ESI-MS/MS analysis.

The sample preparation method was evaluated by considering the trueness and repeatability of five spiked ultrapure water (18.2 MΩ) samples with a native L- and D-amino acids solution (average concentration 1 μg L^{-1}) and an isotopically-labeled ^{13}C-amino acids solution (average concentration of 1 μg L^{-1}). The accuracy of the spiked samples relative to the standard, ranged from −1 % (L-Ala) to 8 % (L-Arg); repeatability, estimated as the relative standard deviation of the five samples, was always below 10 %.

The determination of free L- and D-amino acids in SLW water and pore water samples was conducted using a method previously developed for these compounds in other Antarctic lakes (Barbaro et al., 2017). Briefly, an Agilent 1100 Series HPLC System (Waldbronn, Germany) was coupled with an API 4000 Triple Quadrupole Mass Spectrometer (Applied Biosystem/MSD SCIEX, Concord, Ontario, Canada) using an electrospray source that operated in positive mode by multiple reaction monitoring (MRM). Chromatographic separation was performed using a 2.1 mm × 250 mm CHIROBIOTIC TAG column (Advanced Separation Technologies Inc., USA) with a mobile phase gradient elution consisting of ultrapure water with 0.1 % formic acid (eluent A) and methanol with 0.1 % formic acid (eluent B). The binary elution gradient program with a flow rate of 0.2 mL min^{-1} was used as follows: 0–15 min, 30 % of eluent B; 15–20 min, gradient from 30 to 100 % B; 20–25 min, 100 % of eluent B; 27–30 min, 30 % eluent B. 100 μL were injected.

The determination of PC (vanillic acid, vanillin, acetovanillone, homovanillic acid, syringic acid, syringaldehyde, ferulic acid, coniferyl aldehyde and p-coumaric acid) was conducted using HPLC (Agilent 1100 Series HPLC Systems) coupled to an API 4000 Triple Quadrupole Mass Spectrometer using an electrospray source that operated in negative mode. Data were collected in MRM mode and the mass spectrometer parameters were the same used in our previous method (Zangrando et al., 2013). Our previous method was integrated with the MRM transitions of acetovanillone with a declustering potential of −46 V and an entrance potential of −10 V: 164.8/149.8 (−19 V and −10 V as collision energy and cell exit potential, respectively) and 164.8/121.7 (−30 V and −9 V as collision energy and cell exit potential, respectively). For chromatographic analysis, 100 μL of sample were injected into a C18 Synergy Hydro column (2.1 mm i.d. x 30 mm length, 4 μm particle size, Phenomenex, Torrance, CA) with an elution flow of 200 μL min^{-1}. The mobile phase A was a 0.01 % formic acid water-based solution and B was a solution of methanol/acetonitrile 80/20. The binary elution program was as follows: 0–1 min, 20 % mobile phase B; 1–6 min, linear gradient from 70 % to 100 % mobile phase B; 6–8 min, washing column with 100 % mobile phase B; 9–16 min, equilibration with 20 % mobile phase B.

FAA and PC quantification was performed using the internal standard method to account for signal fluctuations and random errors during the sample treatment (Boyd et al., 2011).

A supporting analysis was carried out to evaluate the presence of levoglucosan, a key tracer of biomass burning. Levoglucosan analysis was

Table 2
REE concentrations in SLW porewater samples. The mean value for acidified filtered CAST samples 1 and 3 (SLW) is reported for comparison. The minus (−) values in the left-hand column indicate sediment depth in cm. Relative standard deviation (RSD) is <5 % except for Ho, Tm and Lu, where 5 % < RSD < 8 %. Ce anomaly, (Ce/Ce*) was calculated as Ce/(La x2/3 + Nd x1/3); Eu anomaly, (Eu/Eu*) was calculated as Eu/(0.5 x Sm + 0.5 x Gd).

	REE (pmol L^{-1})																		Anomalies[d]	
	La	Ce	Pr	Nd	Sm	Eu	Gd	Tb	Dy	Ho	Er	Tm	Yb	Lu	ΣREE	ΣLREE[a]	ΣMREE[b]	ΣHREE[c]	Ce/Ce*	Eu/Eu*
0SLW0	373.8	787.2	90.9	317.5	188.6	17.8	61.7	8.6	45.2	11.4	25.3	3.7	24.3	4.3	1960.3	1569.5	333.3	57.6	1.05	0.78
−1	171.1	339.9	219.7	753.0	535.9	12.4	20.9	22.4	13.8	2.6	6.3	4.7	30.3	2.2	828.9	675.8	139.8	13.4	1.04	1.27
−3	140.8	190.7	155.8	469.3	296.9	7.9	6.5	9.2	7.0	0.9	2.5	2.7	10.8	1.6	514.9	437.4	71.6	5.9	0.77	1.62
−5	197.9	343.1	211.1	785.7	465.7	10.4	19.5	18.2	15.6	2.9	7.0	5.6	35.8	2.0	851.1	709.8	126.5	14.9	0.94	1.21
−9	160.9	312.9	208.9	688.1	478.2	10.5	16.7	15.7	11.0	2.7	5.0	4.0	27.1	1.8	757.5	625.8	120.6	11.2	1.03	1.24
−13	323.5	507.7	359.6	1037.1	661.2	9.3	15.2	19.7	13.0	3.1	5.2	3.9	31.9	1.7	1230.7	1068.0	150.6	12.0	0.9	0.86
−15	29.3	71.8	32.4	114.3	76.3	4.9	5.0	4.2	2.9	1.0	1.1	2.1	7.3	1.1	156.3	126.0	26.8	3.6	1.33	3.04
−17	31.6	47.4	34.4	116.6	105.6	4.4	3.6	5.4	2.0	1.8	1.3	2.8	7.1	1.3	138.2	104.6	29.6	4.0	0.83	2.37
−19	155.2	235.7	150.1	591.4	420.7	8.8	11.8	14.3	10.6	2.8	3.3	2.6	19.8	2.1	629.1	516.5	104.2	8.5	0.83	1.23
−21	65.1	85.9	60.0	206.7	170.9	7.1	6.2	8.2	4.0	2.6	1.8	2.6	13.8	1.5	250.6	196.1	48.9	5.6	0.76	2.33
−23	54.3	67.6	41.0	152.8	129.8	5.0	4.4	9.1	2.9	2.2	2.0	2.0	10.8	1.4	196.7	154.7	36.8	5.2	0.74	2.19
−25	54.9	77.5	42.5	190.4	154.9	5.6	5.0	6.3	4.7	2.2	2.0	1.1	11.0	1.4	220.4	171.8	43.5	5.1	0.79	2.08
−29	73.3	60.9	45.8	178.9	154.6	5.0	3.9	5.7	1.9	3.7	1.7	2.7	6.4	1.3	216.9	172.2	40.4	4.2	0.51	1.92
−31	184.3	245.0	165.1	641.9	401.0	8.3	13.0	13.9	9.1	3.8	3.6	2.9	19.2	2.2	676.0	565.9	101.1	8.9	0.64	1.18
−33	94.9	110.7	79.2	273.0	161.5	5.2	6.2	7.5	3.2	4.0	2.5	3.0	14.9	2.0	318.3	265.3	45.9	7.1	0.69	1.79
−35	67.4	68.5	19.6	91.2	103.7	5.3	3.2	4.3	2.3	2.4	1.4	1.7	4.4	1.3	188.7	154.6	30.5	3.5	0.68	2.96
−37	139.3	144.0	44.6	179.1	142.3	5.4	4.9	8.2	3.7	3.6	0.9	1.7	11.8	1.2	367.1	321.2	41.9	4.0	0.28	2.16

[a] Average of La, Ce, Pr, Nd.
[b] Average of Sm, Eu, Gd, Tb, Dy, Ho.
[c] Average of Er, Tm Yb, Lu.
[d] PAAS normalized ratios.

performed using a method specifically developed for the analysis of polar ice samples (Gambaro et al., 2008) based on the same HPLC -MS/MS previously used for PC analysis. Briefly, chromatographic separation was obtained using a C18 Synergi Hydro column (4.6 mm i.d., 50 mm length, 4 μm size particles; Phenomenex, Torrance, CA). The samples were eluted with methanol (ultragradient, H411, Romil Ltd., Cambridge, UK) and ultrapure water (18.2 MΩ, TOC 1 ppb, PURELAB Pulse and PURELAB Flex, Elga). The MS was equipped with an ion spray source ((−)ESI) Turbo V operating in negative polarity. Mass / charge (m/z) ratios used for the quantification were 161 and 113 for levoglucosan and 167 and 118 for ^{13}C-labeled levoglucosan.

2.5. Statistical methods

To better evaluate all the data together a statistical approach is used. A Principal Component Analysis (PCA) were performed to highlight the relationship between inorganic and organic components. The PCA was done using RStudio, Version 1.0.153 (RStudio-Team, 2015). PCA is a technique for reducing the dimensionality of datasets, minimizing information loss, and increasing interpretability of data.

Also some correlation coefficients are reported to highlight the correlation between pairs of analytes, and p-value from both paired and unpaired t-test. The t-test helps us to test the significance of our hypothesis, i.e. whether the difference between the two datasets considered is a true difference or is a casualty.

3. Results and discussion

REE, TE, FAA, and PC concentration in the water column and in porewater are discussed here to (i) determine the type and sources of inorganic components and organic matter in the water column and sediment porewater of SLW and, (ii) highlight the response of certain redox-sensitive elements to the observed redox changes in the sediments.

3.1. REE concentrations and potential sources

The REE concentrations for both the unfiltered and filtered samples in the borehole cast were similar, indicating that REE concentrations were not influenced by particulate/colloidal material (Table 1). In contrast, the filtered lake samples had at least an order of magnitude higher REE concentrations than those measured in the borehole, and the unfiltered samples a further two orders of magnitude higher concentrations than those measured in the borehole (Table 1). These data reveal that borehole water from drilling had little impact on the lake water geochemistry. The porewater (filtered) REE concentrations were up to an order of magnitude lower than the filtered lake water concentrations (Table 2). This difference may be related to the high level of colloidal material in the lake waters (Fig. S1) that could be solubilized during the 24 h nitric acid treatment during sample preparation. REE concentrations within the pore water samples was higher in the upper part of the sediment profile. Specifically, the average (± SD) concentration of ΣREE from −1 to −13 cm was 836.3 (± 257.5) pmol L^{-1} and from −15 to −37 cm, 305.3 (± 184.3) pmol L^{-1} (Table 2). This pattern was observed in each of the elemental groups: ΣLREE (light REE, La to Nd), ΣMREE (intermediate REE, Sm to Ho) and ΣHREE (heavy REE, Er to Lu).

The relative fractionation of REE is typically normalized with respect to reference values, such as the Post Archean Australian Shale (PAAS), North American Shale Composite (NASC), World Shale Average (WSA) or the Upper Continental Crust (UCC). The REE data in our study were normalized to the Post Archean Australian Shale (PAAS) (Pourmand et al., 2012; Piper and Bau, 2013). The normalization to a shale provides an estimate of the REE abundance relative to that of the continental crust. A flat pattern

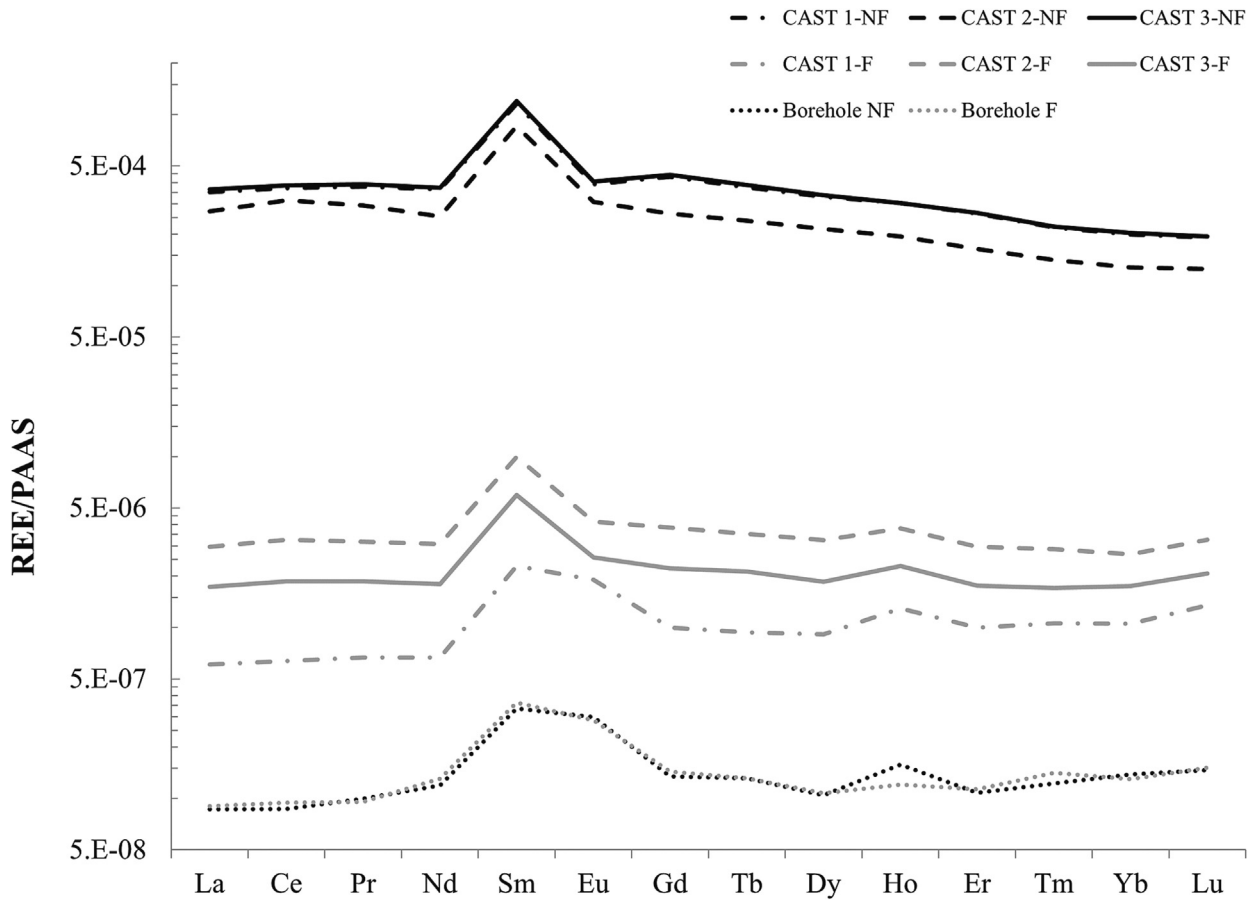

Fig. 2. PAAS normalized pattern of REEs for borehole and SLW lake water samples. NF denotes unfiltered samples and F, filtered samples.

indicates a composition similar to that of continental crust (Byrne and Sholkovitz, 1996). The PAAS normalized patterns of REEs for the borehole and lake waters whether filtered or unfiltered were broadly similar, showing relatively little change in the elements relative abundances measured across all samples (Fig. 2). The PAAS normalized pattern of REEs in the sediment porewaters also showed relatively small changes in the normalized abundances measured over depth (Fig. 3) indicating no major changes in sedimentary sources, weathering processes and relative mobility, but also an evolution of porewater's geochemical characteristics with depth probably related to dynamic of the subglacial lake.

3.2. Trace elements and REE in sediment porewaters

The trace elements Fe, Ba, Cr, V, Mn and Sr in sediment porewater varied with depth (Fig. 4, Table 3). Specifically, Cr and V decrease in concentration with depth, with a marked change in the concentration profile shape of V at −15 cm depth. Sr and Mn both showed increasing concentration with increasing depth in the sediment. Fe and Ba fluctuated around relative consistent average values with increasing depth, with Fe concentrations higher variability around the mean value; Fe, 200.1 ± 112.8 nmol L^{-1} and Ba, 87.2 ± 11.7 nmol L^{-1} (Fig. 4). The decrease in Vanadium concentration with depth has been interpreted to indicate a decreasing oxygen concentration in the sediment porewaters (Michaud et al., 2016) given that it is redox sensitive (Morford and Emerson, 1999). As dissolved oxygen decreases, V is reduced and removed via precipitation (Morford and Emerson, 1999). The evident decrease of V at a depth below 15 cm infers decreasing oxygen concentration. The concentration profile of Mn and Sr in the sediment porewaters is similar to that of chloride (Michaud et al., 2016), where these authors concluded that there was a seawater source in the sediments below the lowest measured depth interval (−36 to −38 cm). The concentration of Ba was higher in the 0 to −15 cm interval (mean value 96 ± 10 nmol L^{-1}) than in the −15 to −37 cm one (mean value 83 ± 11 nmol L^{-1}), and the relevance of this difference is highlighted by an unpaired *t*-test whose *p*-value is =0.018. Considering that, generally, the barium concentration in water is controlled by the amount of sulfate ion and that, as reported by Michaud et al. (2016), sulfate ions increase with depth in SLW samples, with a trend similar to that of Cl^-, it is possible to hypothesize a seawater influence for Ba in porewater samples. On the other hand, Ba profile could also be related to a reductive dissolution of Mn oxides that, in conjunction with changes in salinity, may also be an important process in maintaining high concentrations of Ba in the pore water (Charette and Sholkovitz, 2006). In this case, it is to expect an increase of Ba below −15 cm, where a suboxic zone was recognized and Mn show an increase in concentration, but there is no evidence of higher Ba levels below this depth, so the seawater influence is to be considered the most important

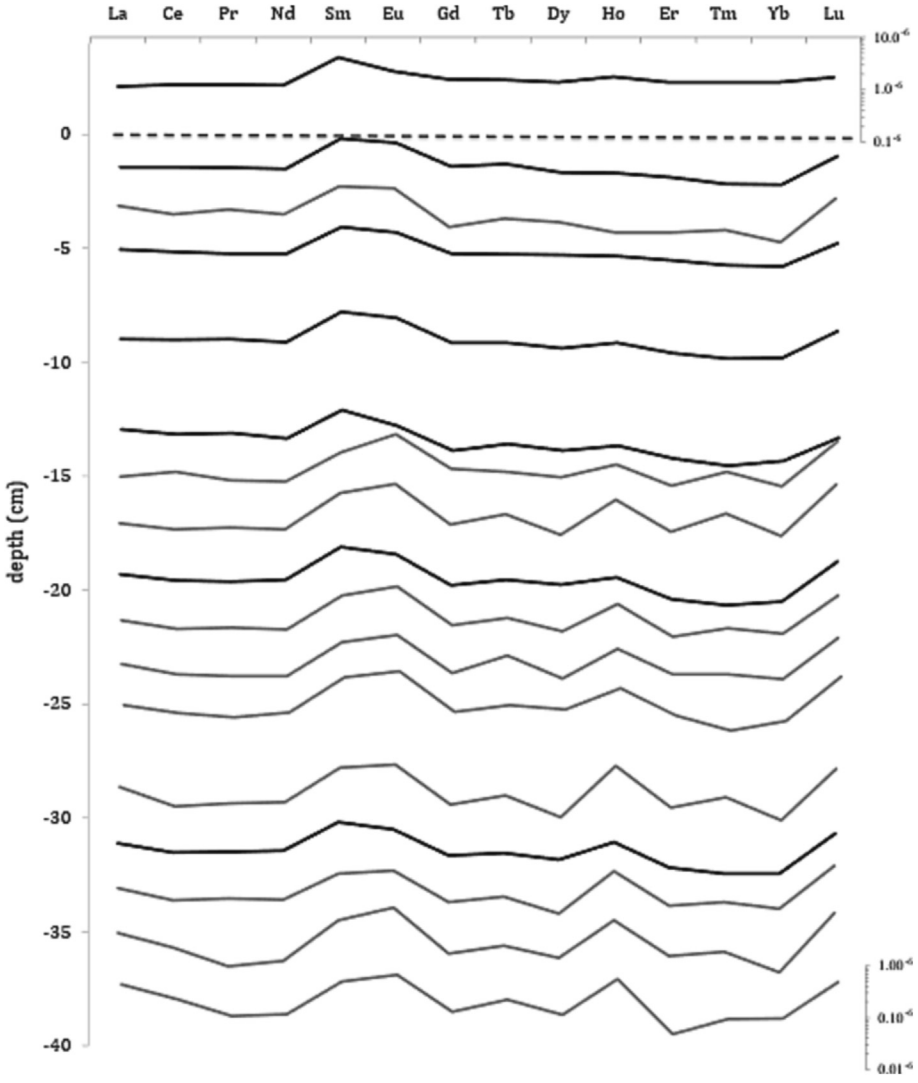

Fig. 3. PAAS normalized pattern of REEs for SLW lake water and sediment porewater. The uppermost line is the SLW lake water value, which is the average of the CAST 1 and CAST 3 filtered sample values. Left vertical scale represents the sample depth in cm; dashed line represents sediment-water interface. Vertical logarithmic scale for black-line patterns is from 0.1^{-6} to 10^{-6}, and for grey-line patterns is from 0.01^{-6} to 1^{-6}. The log-scale on the right side for SLW lake water and for −37 cm depth samples are shown as examples.

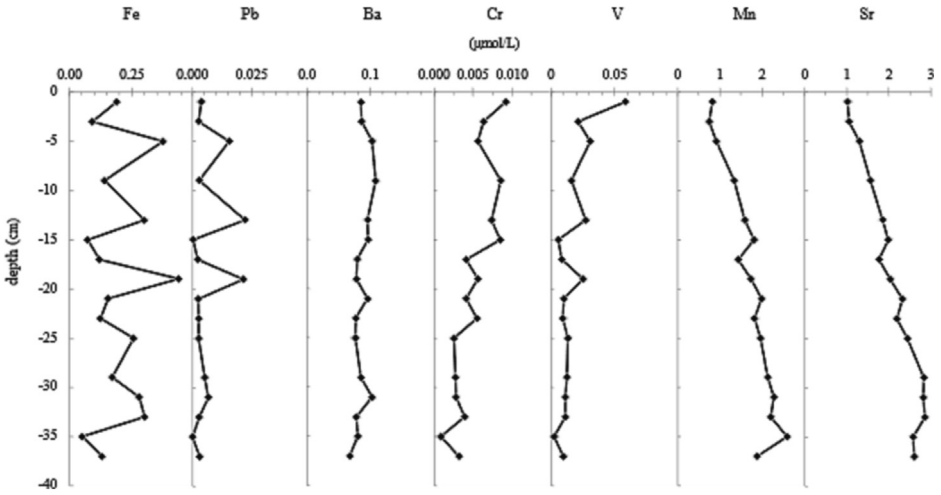

Fig. 4. SLW sediment porewater depth profiles of Fe, Pb, Ba, Cr, V, Mn and Sr.

factor in Ba distribution. The concentration of Fe presumably remains relatively constant with depth because of the oxidized nature of the sediments and because our method does not distinguish between Fe^{2+} and Fe^{3+}; hence, the redox sensitivity of Fe2+ from porewaters is lost. Nonetheless, some consideration about Fe speciation can be done on the basis of the lead (Pb) profile. Pb is not a redox active element. However, when redox conditions change common Pb hosts, including Fe hydroxide, dissolve and precipitate releasing Pb to porewater. This change could cause the spikes in dissolved Pb concentration (Dewey et al., 2021) that broadly correlate with dissolved Fe.

The relationship between trace elements and REE is not well characterized in lake sediment porewaters (Manasypov et al., 2021). La, Gd and Yb representative of LREE, MREE and HREE, respectively, were plotted with depth along with the Ce and Eu anomaly values to examine this relationship (Fig. 5). Ce and Eu anomalies were calculated as $Ce/Ce^* = 3Ce/(2La + Nd)$ and $Eu/Eu^* = 2Eu/(Sm + Gd)$ respectively. Porewater REE profiles showed elevated concentrations in the upper 15 cm, with much lower average values at depths from −15 to −37 cm. This is similar to the behaviour of Vanadium (V) (Fig. 4). Whether these changes in REE concentrations are related to the redox condition remains unknown, but the data imply that higher REE concentrations are correlated with more oxic conditions (the correlation coefficients between LREE-MREE-HREE and V is respectively 0.67-0.78-0.78, while *p*-value, obtained from a pared *t*-test, is well below 0.05 indicating that this correlation is not casual). Similar to the La, Gd and Yb concentration profiles, the Ce anomaly shows higher mean values in the upper 15 cm relative to those for 15 cm and below (p-value = 0.044 indicates a significant difference) while Eu anomaly shows lower mean values in the upper 15 cm relative to those for 15 cm and below (p-value = 0.001 indicates a significant difference). These changes in the Ce and Eu anomalies are also partially correlated with the inferred redox state of the sediment profile using V (both for Ce and Eu anomalies the t-test shows a p-value well below 0.05 [$1.2*10^{-9}$ and $1.2*10^{-8}$ respectively]) but we have no simple geochemical explanation for this relationship. In particular, the Eu anomaly is negatively well correlated with V (correlation coefficient = −0.66) while the Ce anomaly shows a weak positive correlation with V (=0.33), but also a negatively good correlation with Sr (= −0.60). Considering that in our samples the Ce anomaly is increasingly negative (defined as <1.00) with depth (ranging from value 0.83 in sample −17 cm, to value 0.28 in sample −37 cm) and it is negative in seawater, the negative correlation with Sr could be related to a seawater source hypothesized in the sediments below the lowest measured depth (Michaud et al., 2016) and found to be present deep in the sediments beneath SLW (Gustafson et al., 2022). Samarium (Sm) shows a peak that characterized both the lake water and the porewater samples where it is higher, with respect of Eu, in surficial samples (−1, −5, −9, −13) and in sample at −19 and −31 cm than in all other samples (Fig. 2). Samples −1, −5, −9, −13, −19, and −31 are also those samples that have higher REE concentration. We do not have any particular explanation for this peak in lake water, but it is evident also in porewater where, however, other sources and/or processes seem to have importance in defining the profile of REE. Specifically, it is to note a peak of Eu that increases in porewater from the top to the bottom and, at less extent of Ho that appears below −15 cm and increases toward the bottom of the core. These peaks could be related both to the sediment and to marine source (a peak of Ho was detected in present-day seawater of the Ross Sea and of South Australia basin (Turetta et al., 2017; Nozaki and Alibo, 2003)). In Fig. 2 it is also evident that the REE profile of depths −19 and −31 are close to the profiles of more oxygenated zone (−1, −5, −9 and −13) showing the same level of concentration and the same peak of Sm higher than the peak of Eu.

3.3. Free amino acids and phenolic compounds in the borehole and SLW water column

L- and D-FAA were determined in SLW water ($n = 3$) and borehole water ($n = 1$) samples, but only four free L-amino acids (L-Ala, L-Arg, L-Phe and L-Pro) had concentrations higher than the method detection limits

Table 3
TE concentrations in porewater samples. The mean value for acidified filtered CAST samples 1 and 3 (SLW) is reported for comparison. The minus (−) values in the left-hand column indicate sediment depth in cm. RSD was <10 % for Ba, Fe and Sr and <5 % for Pb, V, Cr and Mn.

	TE						
	(nmol L^{-1})				(µmol L^{-1})		
	Ba	Pb	V	Cr	Mn	Fe	Sr
SLW	52.6	0.11	47.3	0.16	0.28	0.03	0.84
−1	85.2	3.80	58.2	9.21	0.82	0.19	1.02
−3	85.8	2.61	21.4	6.35	0.75	0.09	1.05
−5	102.6	15.62	30.8	5.64	0.92	0.38	1.29
−9	108.4	2.96	16.2	8.57	1.35	0.14	1.57
−13	95.5	22.14	27.2	7.37	1.60	0.30	1.85
−15	96.5	0.35	5.8	8.49	1.80	0.07	1.99
−17	79.9	2.27	8.5	4.10	1.44	0.12	1.76
−19	77.9	21.52	25.1	5.61	1.74	0.44	2.04
−21	95.7	2.49	10.2	4.13	1.98	0.16	2.33
−23	76.9	2.72	9.2	5.49	1.82	0.12	2.19
−25	76.0	2.61	13.3	2.56	1.97	0.26	2.44
−29	84.9	5.18	12.3	2.78	2.14	0.17	2.83
−31	103.0	6.69	11.1	2.84	2.28	0.28	2.82
−33	78.3	2.85	11.4	3.91	2.21	0.30	2.86
−35	80.5	0.19	2.4	0.87	2.59	0.05	2.57
−37	67.4	3.18	9.8	3.22	1.88	0.13	2.60

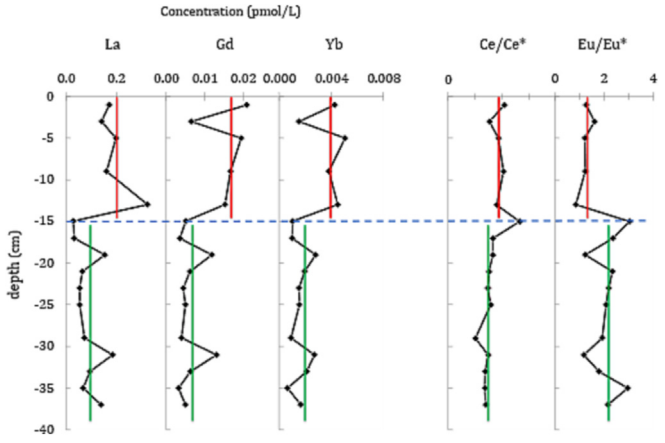

Fig. 5. SLW sediment porewater depth profiles of La, Gd and Yb representative of LREE, MREE, and HREE respectively, Ce anomaly (Ce/Ce*), and Eu anomaly (Eu/Eu*). Note a clear change in the concentration profile at 15 cm depth for La, Gd and Yb as well as for the Ce and Eu anomalies. The red bars represent the mean value above 15 cm depth, while the green bars represent the mean value below 15 cm depth.

(MDLs), while all D-amino acids were below MDLs (Fig. 6), which is not surprising as D-enantiomers usually contribute <10 % to total FAA concentration in sea-waters (Wedyan and Preston, 2008). The total concentration of FAA was 12 and 13 (±3) nM in borehole and SLW water (Fig. 6), respectively. These are approximately an order of magnitude lower than the only other measurements of total amino acids (sum of bound and free amino acids) from Subglacial Lake Vostok, where concentrations in the accreted ice were >100 nM (Christner et al., 2006). Note that when accreted ice forms, solute is rejected from the ice and thus the concentration of the amino acids in Subglacial Lake Vostok, will be higher than in the accreted ice (Christner et al., 2006; Santibáñez et al., 2019). The FAA concentrations in SLW were also lower than those in Antarctic lacustrine waters where photosynthetic primary production occurs (Gibson et al., 1994: 48–268 μM; Barbaro et al., 2014: 0.1–8.5 μM). These data suggest organic matter, especially an important biomass precursor, like amino acids, are likely tightly regulated and taken up from the SLW water column if released to the water through cell lysis.

Vanillic acid and vanillin were the only lignin degradation products found in borehole and SLW water (Fig. 6). The mean concentrations of vanillin were 0.18 nM and 0.22 (±0.06) nM in borehole (CAST-N) and SLW water samples, respectively. Vanillic acid was less abundant in borehole and lake samples, with mean concentrations of 0.13 nM and 0.06 (±0.01) nM. In general, vanillin is one of the products of biological lignin degradation by fungi and can be further oxidized to vanillic acid (Flaig, 1964). Previous studies on dissolved vanillin in estuarine ecosystems reported concentrations of this compound >1 nM (Dittmar et al., 2001; Edelkraut, 1996; Motamed and Texier, 2000; Opsahl and Benner, 1998; Reeves and Preston, 1989). Edelkraut (1996) focused on free dissolved vanillin to test whether such measurements yield information on terrestrial carbon inputs into an estuarine system and on the vanillin derived from lignin oxidation. The main conclusion of Edelkraut (1996) was that vanillin is most likely released by microbial degradation of lignin and not by the distribution of lignin-containing material. Our data suggest that lignin degradation did not occur in SLW, and it is plausible due to the lack of and distance from any vascular plants.

The borehole sample is comprised of ice melt and some snowmelt (hot water drilling fluid), therefore, the low, but similar concentration of vanillic acid and vanillin in the borehole and SLW samples suggest that the source of these compounds to SLW is primarily ice melt. The sources for the phenolic compounds in ice melt could be from microbial degradation of lignin and/or biomass burning. Vanillic acid from biomass burning has been detected in an ice core from the West Antarctic Ice Sheet (Saltzman et al., 2014). However, the concentration of levoglucosan, a key tracer of biomass burning, in the borehole and SLW samples were below the MDL (20 pg mL^{-1}) indicating that combustion products of biomass burning are less likely as a source of phenolic compounds, but it is noted that levoglucosan can degrade rapidly (Hennigan et al., 2010).

3.4. Indicators of organic matter sources in sediment porewater: free amino acids and phenolic compounds

The L-amino acids (L-Ala, L-Arg, L-Asp, L-Leu, L-Orn, L-Thr, L-Tyr, L-Val) and glycine, were detected in all sediment porewater samples (Fig. 7). The average total concentration of FAA in the porewater was 650 nM (range = 36–2957 nM) which is higher than the concentration in bulk SLW water (13 nM). However, these FAA concentrations are at the lower end of the range (0.4–200 μM) reported in the porewaters of sediments from rivers, bays or fjords (Colombo et al., 1998 and references therein), suggesting low inputs of organic carbon and microbial biomass. The amino acid concentrations were relatively consistent with depth (Fig. 7), with peaks at −5 and −23 cm for all compounds and one peak of glycine also at −31 cm. L-Orn and Gly were the most abundant compounds in the porewater (30 % and 25 %) and high percentages were detected also for L-Ala (13 %) and L-Asp (14 %). L-Ala and L-Arg were detected in both samples (lake water and porewater) while L-Phe and L-Pro were below the MDL in the porewater samples. High correlation coefficients among amino acids in porewater profiles (> 0.7) suggest that the major source(s) for each compound in the porewaters was likely the same.

Amino acids in pore water samples may have numerous sources and sinks. These may include excretion and incorporation by living organisms or abiotic transformation (e.g. dehydration, racemization). Therefore, amino acids can be recycled several times before eventually ending up as inorganic nitrogen or macromolecular humic substances (Jorgensen,

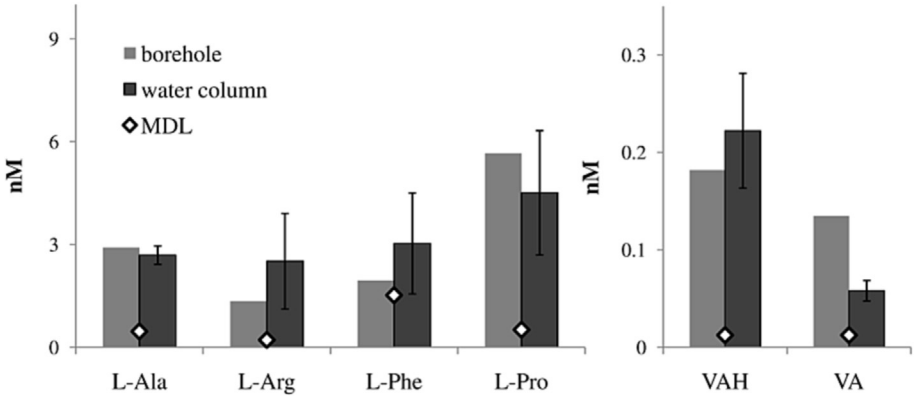

Fig. 6. Mean concentrations of free amino acids and phenolic compounds (vanillic acid, VA, and vanillin, VAH) in the SLW lake water column and in the borehole. Method detection limits (MDLs) are reported for each compound.

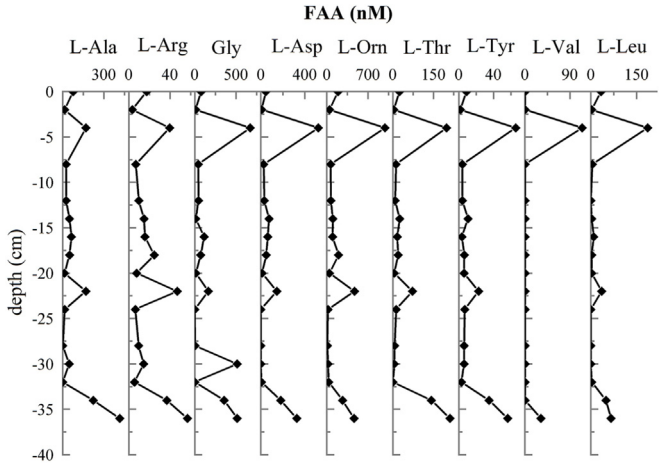

Fig. 7. Depth concentration profiles for each amino acid (nM) in SLW sediment porewater.

1982; Stanley et al., 1987). Considering previous results (Christner et al., 2014; Achberger et al., 2016; Purcell et al., 2014; Vick-Majors et al., 2020b) that confirmed the presence of a diverse, active assemblage of bacteria and archaea in SLW, it is plausible that amino acids in the porewater might be released from bacteria, which are the key factor for solubilising POM (particulate organic material) and recycling of labile DOM (dissolved organic material) in lacustrine environments (Schweitzer et al., 2001). The FAA in the porewaters likely provide a source of energy and nitrogen for microorganisms due to their ability to efficiently use dissolved organics (Stanley et al., 1987) and the low concentrations suggest a limited source or tight cycling within the SLW water column.

The syringyl, vanillyl and cinnamyl phenols vanillic acid (VA), vanillin (VAH) and acetovanillone (VAC) were detected in sediment porewater with an average concentration for the sum of all three compounds, of 70 nM (16–167 nM) (Fig. 8). The concentrations in the porewater samples were considerably higher than those in the lake water column (0.3 nM as sum of lake water VA and VAH), excluding the latter as a possible source of PC in porewater. Vanillyl phenols are products of biomass burning (Zangrando et al., 2013 and references therein) or degradation of vegetation (Dittmar et al., 2001; Edelkraut, 1996). Levoglucosan is a key tracer of biomass burning (Zangrando et al., 2013), but levoglucosan concentrations were below the detection limits for SLW water and sediment porewater samples indicating that biomass burning is not the source of PC in the SLW porewaters. Further, the concentration of vanillic acid in the porewaters is orders of magnitude greater that those reported in

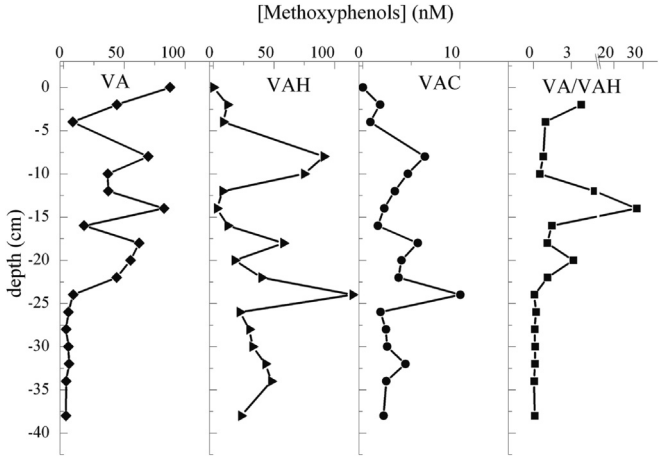

Fig. 8. Depth profile of methoxyphenols (nM) in SLW sediment porewaters. Vanillic acid, VA, vanillin, VAH and acetovanillone, VAC.

(Arctic) ice cores (e.g. Grieman et al., 2018). Vanillyl phenols are also produced by the degradation processes of vascular plants (Hedges and Mann, 1979) and are considered refractory components because they are typically more concentrated in sediments (Charriére et al., 1991). Syringyl phenols are more susceptible to degradation than vanillyl phenols (Hedges and Mann, 1979). For this reason, the absence of syringyl compounds in our SLW porewater samples does not exclude the presence of other types of plant residues. The vanillyl phenols in the SLW porewaters could be from terrestrially-derived organic matter. If so, this would imply an ancient source for this organic matter, potentially from the last interglacial or earlier. This conclusion is consistent with the findings of Neuhaus et al. (2021) who reported that the bulk of the sedimentary organic matter in SLW was likely from pre-glacial terrestrial C3 plants rich in recalcitrant components such as cellulose, lignin, or sporopollenin.

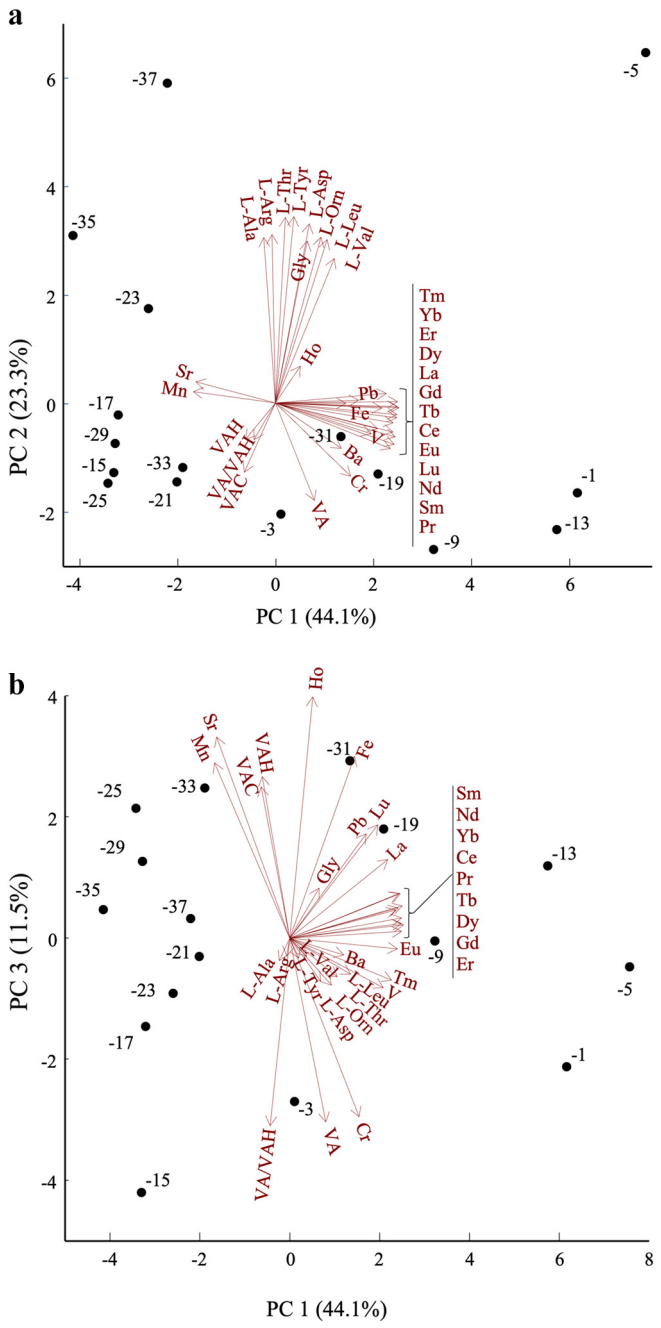

Fig. 9. Biplot of Principal Component (PC) 1 vs. PC 2 (a) and vs PC 3 (b): organic compounds, TE and REE in sediment porewater samples are analysed. In parenthesis the explained variance.

The analysis of lignin degradation potentially provides information on diagenesis as lignin is relatively resistant to breakdown and therefore persists in the sedimentary record longer than other forms of primary organic matter (Meyers and Ishiwatari, 1993). In addition, the acid-to aldehyde (VA/VAH) ratio of vanillyl phenols indicate the extent of the microbial degradation of organic matter (Hedges et al., 1988). Vanillin concentrations increased with depth in the sediments as oxygenation decreased below 15 cm, while vanillic acid concentrations were higher in the more oxygenated surface sediments (Fig. 8). Vanillic acid is the more oxidized component and its elevated concentration indicates oxidative degradation of lignin. Goñi et al. (1993) showed that when the acid-to-aldehyde (VA/VAH) ratio is above 0.4 it is indicative of oxidative degradation. In our samples, VA/VAH values ranged between 0.8 and 28 in the upper 23 cm with a median value of 1.4, while deeper samples had a VA/VAH mean value of 0.08. The VA/VAH ratio reveals that the upper 23 cm exhibit oxidizing conditions, with an evident peak in VA/VAH at 14 cm. This is apparently in contrast with the indication of oxidation based on redox-sensitive elements (e.g. V). However, the extent of oxidative degradation and thus the VA/VAH ratio depends on a variety of factors including the types of organisms responsible for degradation (e.g. bacteria) in addition to the oxygen concentration (Opsahl and Benner, 1995).

3.5. Principal component analysis (PCA)

We performed a PCA to highlight the relationship between inorganic and organic components. The PCAs were performed using RStudio, Version 1.0.153 (RStudio-Team, 2015). Principal component analysis (PCA) is a technique for reducing the dimensionality of datasets, minimizing information loss, and increasing interpretability of data.

The PCA was done considering TE (Ba, Cr, Fe, Mn, Pb, Sr, and V), REE, L-amino acids and vanillyl phenols in porewater samples. Principal Component 1 (PC1) vs. Principal Component 2 (PC2) and PC1 vs Principal Component 3 (PC3) are plotted in Fig. 9a and b respectively. PC1 separates surficial porewater samples (from −1 to −13 cm depth) and two samples at depth, that show higher concentrations of REE all other porewater samples. This separation is principally due to the association of REE, V, Fe, Pb, Cr, and, in less extent, VA as opposed to Mn, Sr, VAC, and VAH. PC2 is principally characterized from the contrast of amino-acids (FAA) with vanillyl phenols, and Cr, and separates those samples with higher amino acid content from all others. Due to their composition PC1 and PC2 could be defined as “prevalent source/sink components”; PC1 seems to represent “inorganic source” while PC2 seems to represent “organic source”. More specifically, PC1 helps separate samples having a marine component (on the negative side of horizontal axis) from all others based on its TE and REE composition. In Fig. 9b, PC1 vs. PC3 are plotted. PC3 is characterized by VA/VAH, VA and Cr (on the negative side of vertical axis) and Mn, Sr, Ho, Fe, VAC, and VAH (on the positive side of vertical axis). Due to association of elements/compounds the PC3 could be defined both as “redox component” and “marine source” that separates samples with specific characteristics. Specifically, the PC3 is strongly characterized, on the positive side, from those elements/compounds already recognized as indicators both of a marine source and of suboxic conditions (see Section 3.2) and, on the negative side, from elements/compounds typically related to more oxic conditions. These associations separate the samples at depth from the surficial ones highlighting their different composition.

To try to extract the most information from the PCA, a ternary diagram was plotted using principal components from 1 to 3 as variables (Fig. 10). Due to the presence of negative values both in loadings and scores, a factor = 0.5 was added to each loading while a factor = 5 was added to each score. In this way the axes at 0 % correspond to maximum negative value of PCs, while the centre of ternary diagram corresponds to 0 value both for loadings and scores. The triangular space let us to visualize the

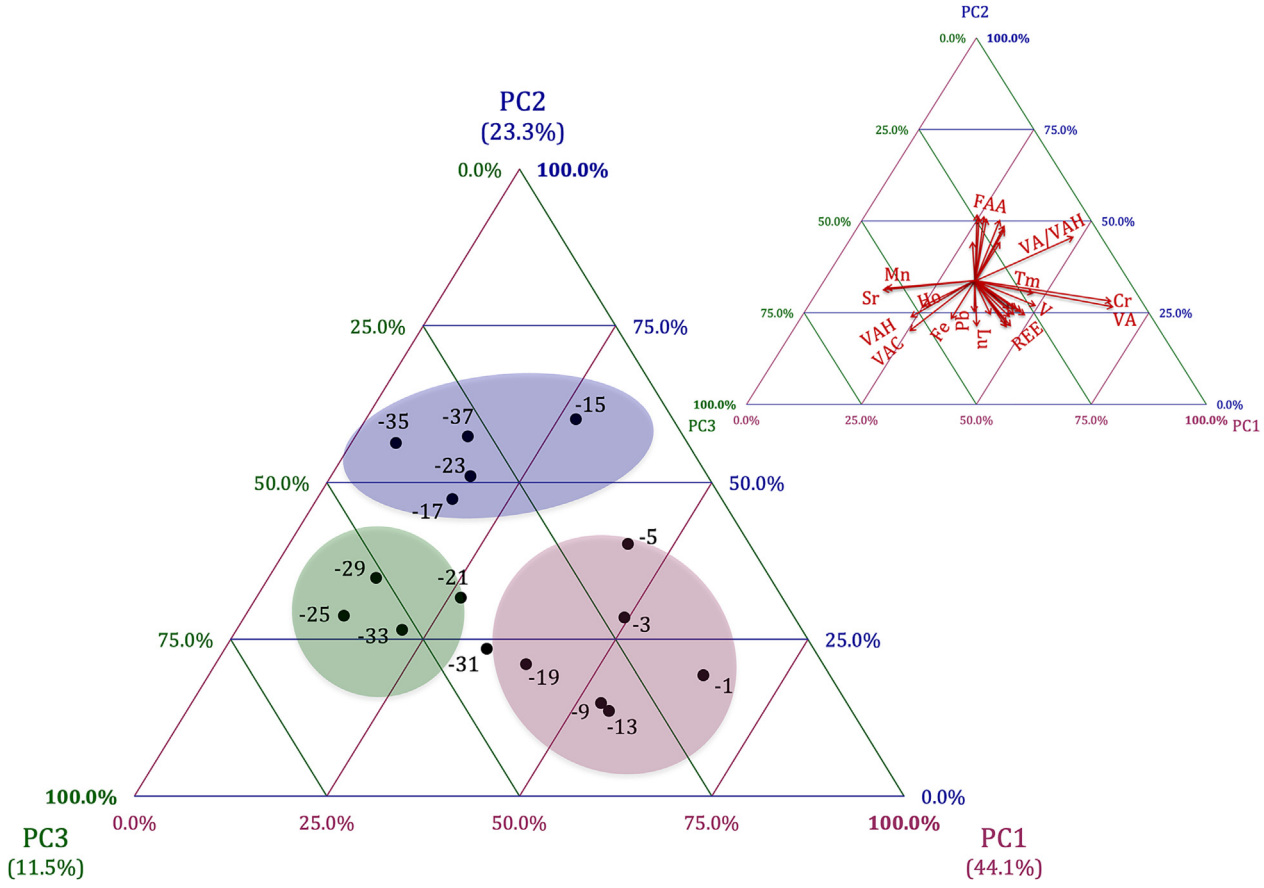

Fig. 10. Ternary diagram of PC1, PC2, and PC3 (in parenthesis the explained variance). The red arrows, in the right-top plot, represent the loadings.

79 % of the variance of data in a single graph. In this graph three groups of samples are recognized. The first group is principally characterized by high values of REE, V, Cr, VA and VA/VAH ratio, the second group is characterized by Sr, Mn, VAC and VAH while the third group is characterized by FAA. The first group joins the surficial samples (−1, −3, −9, and −13), the second the samples −21, −25, −29, and −33, and the third the samples −15, −17, −23, −35, and −37. All these variables together let us to define the bottom right corner as the more oxygenated zone, the bottom left corner as the less oxic area and the top corner as FAA area. Certain samples are placed between these groups revealing the prevalence of a secondary characteristic or the relevance of two different aspects together. Samples −19 and −31 are placed at mid-way between oxic and sub-oxic regions and seem to be strongly characterized by REE, Fe and Pb. This last association places these samples in the suboxic area due to relevance of Pb and Fe, that seems resulting from an oxygen concentration decrease. On the other hand the high concentration of REE, joins these two samples to the surficial ones (−1, −3, −9, and −13), as already highlighted from Sm peak (see Section 3.2 and Fig. 2), and probably related to lake water composition itself. The second and third groups are in the suboxic region and strongly influenced from marine source as highlighted from the association of Sr, Mn and Ho. The third group, that joins together the samples (−15, −17, −23, −35, and −37) with the lowest REE concentration, is characterized from high value of FAA, possibly indicating a different source and/or different patterns of microbial utilization for these samples with respect to all others.

4. Conclusion

We present a suite of detailed geochemical measurements of trace elements and carbon compounds in the water and sediments of a subglacial Antarctic lake. REE, TE, FAA, and PC were detectable in SLW water column and porewater samples collected from a SLW sediment core. Properties and distribution of these compounds demonstrated that: (i) Concentration of REE's and certain redox sensitive TE's do reflect changes in the redox conditions of the sediments, (ii) Free amino acid concentrations are low relative to other freshwater and marine sediments, indicating tight cycling of N-rich compounds, (iii) Vanillyl phenols are present in the sediments, suggesting the presence of ancient terrestrial plant matter, while their concentration profiles may also be related to sediment redox conditions.

Collectively, our results lead us to conclude that SLW is a geochemically complex environment where porewater is influenced both from melt water sourced from the overlying ice sheet and from inputs from past marine incursions.

CRediT authorship contribution statement

Clara Turetta: Conceptualization, Formal analysis, Data curation, Writing – original draft, Investigation. **Elena Barbaro:** Formal analysis, Data curation, Writing – original draft, Investigation. **Mark L. Skidmore:** Investigation, Writing – review & editing. **Andrea Gambaro:** Writing – review & editing. **Alexander B. Michaud:** Investigation, Writing – review & editing. **Andrew C. Mitchell:** Writing – review & editing. **Trista J. Vick-Majors:** Investigation, Writing – review & editing. **John C. Priscu:** Conceptualization, Investigation, Writing – review & editing, Project administration. **Carlo Barbante:** Conceptualization, Investigation, Writing – original draft, Supervision.

Data availability

Data will be made available on request.

Declaration of competing interest

The authors declare that they have no known competing financial interests or personal relationships that could have appeared to influence the work reported in this paper.

Acknowledgements

Support was provided by the Italian National Antarctic Program (PNRA - 2009/A2.02, CaBILA project). The authors thank the WISSARD science team for assistance in project planning and sample collection. The Whillans Ice Stream Subglacial Access Research Drilling (WISSARD) project was funded by National Science Foundation grants (OPP-0838933, 1346250, 1439774). Partial support was provided by graduate fellowships from the NSF-IGERT Program (0654336), Montana Space Grant Consortium and NSF-Center for Dark Energy Biosphere Investigations (A.B.M) and a dissertation grant from the American Association of University Women (T.J.V-M). The authors thank Elga Lab water, High Wycombe UK for supplying the pure water systems used in this study.

Appendix A. Supplementary data

Supplementary data to this article can be found online at https://doi.org/10.1016/j.scitotenv.2023.164480.

References

Achberger, A.M., Christner, B.C., Michaud, A.B., Priscu, J.C., Skidmore, M.L., Vick-Majors, T.J., Adkins, W., Anandakrishnan, S., Barbante, C., Barcheck, G., 2016. Microbial community structure of subglacial Lake Whillans, West Antarctica. Front. Microbiol. 7, 1457.
Ashmore, D.W., Bingham, R.G., 2014. Antarctic subglacial hydrology: current knowledge and future challenges. Antarct. Sci. 26, 758–773.
Barbaro, E., Zangrando, R., Vecchiato, M., Turetta, C., Barbante, C., Gambaro, A., 2014. D-and L-amino acids in Antarctic lakes: assessment of a very sensitive HPLC-MS method. Anal. Bioanal. Chem. 406, 5259–5270.
Barbaro, E., Spolaor, A., Karroca, O., Park, K.-T., Martma, T., Isaksson, E., Kohler, J., Gallet, J.C., Bjorkman, M.P., Cappelletti, D., 2017. Free amino acids in the Arctic snow and ice core samples: potential markers for paleoclimatic studies. Sci. Total Environ. 607, 454–462.
Boyd, R.K., Basic, C., Bethem, R.A., 2011. Trace Quantitative Analysis by Mass Spectrometry. John Wiley & Sons.
Bronk, D.A., Glibert, P.M., Ward, B.B., 1994. Nitrogen uptake, dissolved organic nitrogen release, and new production. Science 265 (5180), 1843–1846.
Byrne, R.H., Sholkovitz, E.R., 1996. Marine chemistry and geochemistry of the lanthanides. In: Gschneidner Jr., K.A., Eyring, L. (Eds.), Handbook on the Physics and Chemistry of Rare Earths Elements. Elsevier, Amsterdam, pp. 497–594.
Carter, S., Fricker, H., 2012. The supply of subglacial meltwater to the grounding line of the Siple Coast, West Antarctica. Ann. Glaciol. 53, 267–280.
Carter, S.P., Fricker, H.A., Siegfried, M.R., 2013. Evidence of rapid subglacial water piracy under Whillans Ice Stream, West Antarctica. J. Glaciol. 59, 1147–1162.
Charette, M.A., Sholkovitz, E.R., 2006. Trace element cycling in a subterranean estuary: part 2. Geochemistry of the pore water. Geochim. Cosmochim. Acta 70 (4), 811–826.
Charriére, B., Gadel, F., Serve, L., 1991. Nature and distribution of phenolic compounds in water and sediments from Mediterranean deltaic and lagunal environments. Hydrobiologia 222, 89–100.
Christner, B.C., Royston-Bishop, G., Foreman, C.M., Arnold, B.R., Tranter, M., Welch, K.A., Lyons, W.B., Tsapin, A.I., Studinger, M., Priscu, J.C., 2006. Limnological conditions in subglacial Lake Vostok, Antarctica. Limnol. Oceanogr. 51, 2485–2501.
Christner, B.C., Priscu, J.C., Achberger, A.M., Barbante, C., Carter, S.P., Christianson, K., Michaud, A.B., Mikucki, J.A., Mitchell, A.C., Skidmore, M.L., Vick-Majors, T.J., Team, W.S., 2014. A microbial ecosystem beneath the West Antarctic ice sheet. Nature 512, 310–313.
Colombo, J., Silverberg, N., Gearing, J., 1998. Amino acid biogeochemistry in the Laurentian trough: vertical fluxes and individual reactivity during early diagenesis. Org. Geochem. 29, 933–945.
Dewey, C., Bargar, J.R., Fendorf, S., 2021. Porewater Lead concentrations limited by particulate organic matter coupled with ephemeral iron(III) and sulfide phases during redox cycles within contaminated floodplain soils. Environ. Sci. Technol. 55, 5878–5886.
Dittmar, T., Lara, R.J., Kattner, G., 2001. River or mangrove? Tracing major organic matter sources in tropical Brazilian coastal waters. Mar. Chem. 73, 253–271.
Dowdeswell, J.A., Siegert, M.J., 1999. The dimensions and topographic setting of Antarctic subglacial lakes and implications for large-scale water storage beneath continental ice sheets. Geol. Soc. Am. Bull. 111, 254–263.
Edelkraut, F., 1996. Dissolved vanillin as tracer for estuarine lignin conversion. Estuar. Coast. Shelf Sci. 43, 737–745.
Elderfield, H., Upstill-Goddard, R., Sholkovitz, E.R., 1990. The rare earth elements in rivers, estuaries, and coastal seas and their significance to the composition of ocean waters. Geochim. Cosmochim. Acta 54, 971–991.
Fisher, A.T., Mankoff, K.D., Tulaczyk, S.M., Tyler, S.W., Foley, N., 2015. High geothermal heat flux measured below the West Antarctic Ice Sheet. Sci. Adv. 1.
Flaig, W., 1964. Effects of micro-organisms in the transformation of lignin to humic substances. Geochim. Cosmochim. Acta 28, 1523–1535.
Fricker, H.A., Scambos, T., 2009. Connected subglacial lake activity on lower Mercer and Whillans ice streams, West Antarctica, 2003 − 2008. J. Glaciol. 55, 303–315.
Fricker, H.A., Scambos, T., Bindschadler, R., Padman, L., 2007. An active subglacial water system in West Antarctica mapped from space. Science 315, 1544–1548.

Fricker, H.A., Powell, R., Priscu, J., Tulaczyk, S., Anandakrishnan, S., Christner, B., Fisher, A.T., Holland, D., Horgan, H., Jacobel, R., 2011. Siple coast subglacial aquatic environments: the Whillans ice stream subglacial access research drilling project. Geophys. Monogr. Ser 194, 199–219.

Gambaro, A., Zangrando, R., Gabrielli, P., Barbante, C., Cescon, P., 2008. Direct determination of levoglucosan at the picogram per milliliter level in Antarctic ice by high-performance liquid chromatography/electrospray ionization triple quadrupole mass spectrometry. Anal. Chem. 80 (5), 1649–1655. https://doi.org/10.1021/ac701655x.

Gibson, J.A., Qiang, X.L., Franzmann, P.D., Garrick, R.C., Burton, H.R., 1994. Volatile fatty and dissolved free amino acids in Organic Lake, Vestfold Hills, East Antarctica. Polar Biol. 14, 545–550.

Goñi, M.A., Nelson, B., Blanchette, R.A., Hedges, J.I., 1993. Fungal degradation of wood lignins: geochemical perspectives from CuO-derived phenolic dimers and monomers. Geochim. Cosmochim. Acta 57, 3985–4002.

Grieman, M.M., Aydin, M., Isaksson, E., Schwikowski, M., Saltzman, E.S., 2018. Aromatic acids in an Arctic ice core from Svalbard: a proxy record of biomass burning. Clim. Past 14, 637–651. https://doi.org/10.5194/cp-14-637-2018.

Gudlaugsson, E., Humbert, A., Kleiner, T., Kohler, J., Andreassen, K., 2016. The influence of a model subglacial lake on ice dynamics and internal layering. Cryosphere 10, 751–760. https://doi.org/10.5194/tc-10-751-2016.

Hedges, J.I., Mann, D.C., 1979. The characterization of plant tissues by their lignin oxidation products. Geochim. Cosmochim. Acta 43, 1803–1807.

Gustafson, C.D., et al., 2022. A dynamic saline groundwater system mapped beneath an Antarctic ice stream. Science 376 (6593), 640–644.

Hedges, J.I., Blanchette, R.A., Weliky, K., Devol, A.H., 1988. Effects of fungal degradation on the CuO oxidation products of lignin: a controlled laboratory study. Geochim. Cosmochim. Acta 52, 2717–2726.

Hennigan, C.J., Sullivan, A.P., Collett, J.L., Robinson, A.L., 2010. Levoglucosan stability in biomass burning particles exposed to hydroxyl radicals. Geophys. Res. Lett. 37, L09806. https://doi.org/10.1029/2010GL043088.

Hodson, T., Powell, R., Brachfeld, S., Tulaczyk, S., Scherer, R., Team, W.S., 2016. Physical processes in Subglacial Lake Whillans, West Antarctica: inferences from sediment cores. Earth Planet. Sci. Lett. 444, 56–63.

Jorgensen, N., 1982. Heterotrophic assimilation and occurrence of dissolved free amino acids in a shallow estuary. Mar. Ecol. Prog. Ser. 8, 145–159.

Livingstone, S.J., Li, Y., Rutishauser, A., Sanderson, R.J., Winter, K., Mikucki, J.A., Björnsson, H., Bowling, J.S., Chu, W., Dow, C.F., Fricker, H.A., McMillan, M., Ng, F.S.L., Ross, N., Siegert, M.J., Siegfried, M., Sole, A.J., 2022. Subglacial lakes and their changing role in a warming climate. Nat. Rev. Earth Environ. 3, 106–124. https://doi.org/10.1038/s43017-021-00246-9.

Manasypov, R.M., Pokrovsky, O.S., Shirokova, L.S., Auda, Y., Zinner, N.S., Vorobyev, S.N., Sergey, N., Kirpotin, S.N., 2021. Biogeochemistry of macrophytes, sediments and porewaters in thermokarst lakes of permafrost peatlands, western Siberia. Sci. Total Environ. 763, 144201.

Meyers, P.A., Ishiwatari, R., 1993. Lacustrine organic geochemistry - an overview of indicators of organic matter sources and diagenesis in lake sediments. Org. Geochem. 20, 867–900.

Michaud, A.B., Skidmore, M., Mitchell, A.C., Vick-Majors, T.J., Barbante, C., Turetta, C., vanGelder, W., Priscu, J.C., 2016. Solute sources and geochemical processes in Subglacial Lake Whillans, West Antarctica. Geology 44, 347–350.

Michaud, A., Vick-Majors, T., Achberger, A., Skidmore, M., Christner, B., Tranter, M., Priscu, J., 2020. Environmentally clean access to Antarctic subglacial aquatic environments. Antarct. Sci. 1 − 12. https://doi.org/10.1017/S0954102020000231.

Morford, J.L., Emerson, S., 1999. The geochemistry of redox sensitive trace metals in sediments. Geochim. Cosmochim. Acta 63 (11/12), 1735–1750.

Motamed, B., Texier, H., 2000. Sources and characteristics of phenolic compounds in the Seine Estuary(France). Oceanol. Acta 23, 167–174.

Neuhaus, S.U., Tulaczyk, S.M., Stansell, N.D., Coenen, J.J., Scherer, R.P., Mikucki, J.A., Powell, R.D., 2021. Did Holocene climate changes drive West Antarctic grounding line retreat and readvance? Cryosphere 15, 4655–4673. https://doi.org/10.5194/tc-15-4655-2021.

Nozaki, Y., Alibo, D.S., 2003. Dissolved rare earth elements in the Southern Ocean, southwest of Australia: unique patterns compared to the South Atlantic data. Geochem. J. 37, 47–62.

Opsahl, S., Benner, R., 1995. Early diagenesis of vascular plant tissues: lignin and cutin decomposition and biogeochemical implications. Geochim. Cosmochim. Acta 59, 4889–4904.

Opsahl, S., Benner, R., 1998. Photochemical reactivity of dissolved lignin in river and ocean waters. Limnol. Oceanogr. 43, 1297–1304.

Piper, D.Z., Bau, M., 2013. Normalized rare earth elements in water, sediments, and wine: identifying sources and environmental redox conditions. Am. J. Anal. Chem. 04 (10), 15.

Pourmand, A., Dauphas, N., Ireland, T.J., 2012. A novel extraction chromatography and MC-ICP-MS technique for rapid analysis of REE, Sc and Y: revising CI-chondrite and Post-Archean Australian Shale (PAAS) abundances. Chem. Geol. 291, 38–54.

Priscu, J.C., Tulaczyk, S., Studinger, M., Kennicutt, M.C., Christner, B.C., Foreman, C.M., 2008. Antarctic subglacial water: origin, evolution, and ecology. In: Vincent, W.F., Laybourn-Parry, J. (Eds.), Polar Lakes and Rivers. Oxford University Press, Oxford, pp. 119–135.

Priscu, J.C., Achberger, A.M., Cahoon, J.E., Christner, B.C., Edwards, R.L., Jones, W.L., Michaud, A.B., Siegfried, M.R., Skidmore, M.L., Spigel, R.H., 2013. A microbiologically clean strategy for access to the Whillans Ice Stream subglacial environment. Antarct. Sci. 25, 637–647.

Priscu, J., Kalin, J., Winans, J., Campbell, T., Siegfried, M., Skidmore, M., Vick-Majors, T.J., et al., 2021. Scientific access into Mercer Subglacial Lake: scientific objectives, drilling operations and initial observations. Ann. Glaciol. https://doi.org/10.1017/aog.2021.10.

Purcell, A.M., Mikucki, J.A., Achberger, A.M., Alekhina, I.A., Barbante, C., Christner, B.C., Ghosh, D., Michaud, A.B., Mitchell, A.C., Priscu, J.C., Scherer, R., Skidmore, M.L., Vick-Majors, T.J., the WISSARD Science Team, 2014. Microbial sulfur transformations in sediments from Subglacial Lake Whillans. Front. Microbiol. 5, 594. https://doi.org/10.3389/fmicb.2014.00594.

Rack, F.R., Duling, D., Blythe, D., Burnett, J., Gibson, D., Roberts, G., Carpenter, C., Lemery, J., Fischbein, S., 2014. Developing a hot-water drill system for the WISSARD project: 1. Basic drill system components and design. Ann. Glaciol. 55, 285–297.

Reeves, A., Preston, M., 1989. The composition of lignin in estuarine suspended particulates and the distribution of particulate lignin in estuaries as determined by capillary gas chromatography of cupric oxide oxidation products. Estuar. Coast. Shelf Sci. 29, 583–599.

Robin, G.d.Q., Swithinbank, C., Smith, B., 1970. Radio echo exploration of the Antarctic ice sheet. Int. Assoc. Sci. Hydrol. Publ. 86, 97–115.

Rosenheim, B.E., Michaud, A.B., Broda, J., Gagnon, A., Venturelli, R.A., Campbell, T.D., SALSA Science Team, 2023. A method for successful collection of multicores and gravity cores from Antarctic subglacial lakes. Limnol. Oceanogr. Methods. https://doi.org/10.1002/lom3.10545.

RStudio-Team, 2015. RStudio: Integrated Development for R. RStudio, Inc., Boston, MA. http://www.rstudio.com/.

Saltzman, E.S., Grieman, M.M., McConnell, J., Cole-Dai, J., 2014. Aromatic acids from biomass burning in the WAIS divide ice core. AGU Fall Meeting Abstracts, pp. C13A–0416.

Santibáñez, Pamela A., Michaud, Alexander B., Vick-Majors, Trista J., D'Andrilli, Juliana, Chiuchiolo, Amy, Hand, Kevin P., Priscu, John C., 2019. Differential incorporation of bacteria, organic matter, and inorganic ions into Lake ice during ice formation. J. Geophys. Res. Biogeosci. https://doi.org/10.1029/2018JG004825.

Schweitzer, B., Huber, I., Amann, R., Ludwig, W., Simon, M., 2001. α-and β-Proteobacteria control the consumption and release of amino acids on lake snow aggregates. Appl. Environ. Microbiol. 67, 632–645.

Siegert, M.J., 2000. Antarctic subglacial lakes. Earth Sci. Rev. 50, 29–50.

Siegert, M., Dowdeswell, J., Gorman, M., McIntyre, N., 1996. An inventory of Antarctic subglacial lakes. Antarct. Sci. 8, 281–286.

Siegfried, M.R., Fricker, H.A., Roberts, M., Scambos, T.A., Tulaczyk, S., 2014. A decade of West Antarctic subglacial lake interactions from combined ICESat and CryoSat-2 altimetry. Geophys. Res. Lett. 41, 891–898.

Siegfried, M.R., Fricker, H.A., Carter, S.P., Tulaczyk, S., 2016. Episodic ice velocity fluctuations triggered by a subglacial flood in West Antarctica. Geophys. Res. Lett. 43 (6), 2640–2648.

Siegfried, M.R., Venturelli, R.A., Patterson, M.O., Arnuk, W., Campbell, T.D., Gustafson, C.D., Michaud, A.B., Galton-Fenzi, B., Hausner, M.B., Holzschuh, S.N., Huber, B., Mankoff, K.D., Schroeder, D.M., Summers, P., Tyler, S., Carter, S.P., Fricker, H.A., Harwood, D.M., Leventer, A., Rosenheim, B.E., Skidmore, M.L., Priscu, J.C., the SALSA Science Team, 2023. The life and Death of a Subglacial Lake in West Antarctica. Geology. Published Online 9 March 2023. https://doi.org/10.1130/G50995.1.

Smith, B.E., Fricker, H.A., Joughin, I.R., Tulaczyk, S., 2009. An inventory of active subglacial lakes in Antarctica detected by ICESat (2003, Äì2008). J. Glaciol. 55, 573–595.

Stanley, S., Boto, K., Alongi, D., Gillan, F., 1987. Composition and bacterial utilization of free amino acids in tropical mangrove sediments. Mar. Chem. 22, 13–30.

Tulaczyk, S., Mikucki, J.A., Siegfried, M.R., Priscu, J.C., Barcheck, C.G., Beem, L.H., Behar, A., Burnett, J., Christner, B.C., Fisher, A.T., 2014. WISSARD at Subglacial Lake Whillans, West Antarctica: scientific operations and initial observations. Ann. Glaciol. 55, 51–58.

Turetta, C., Cozzi, G., Barbante, C., Capodaglio, G., Cescon, P., 2004. Trace elements determination in seawater by ICP-SFMS coupled with a micro-flow nebulization/desolvation. Anal. Bioanal. Chem. 380, 258–268.

Turetta, C., Barbaro, E., Capodaglio, G., Barbante, C., 2017. Dissolved rare earth elements in the central-western sector of the Ross Sea, Southern Ocean: geochemical tracing of seawater masses. Chemosphere 183, 444–453. https://doi.org/10.1016/j.chemosphere.2017.05.142.

Venturelli, R.A., Davis, C., Boehman, B., Christner, B., Fricker, H.A., Galy, V., Gustafson, C., Harwood, D., Leventer, A., Michaud, A., Mosbeux, C., Priscu, J.C., Siegfried, M., Vick-Majors, T.J., Rosenheim, B.E., the SALSA Science Team, 2023. The origin, age, and cycling of carbon in an Antarctic Subglacial Lake. AGU. Advances 4, e2022AV000846. https://doi.org/10.1029/2022AV000846.

Vick-Majors, T.J., Mitchell, A.C., Achberger, A.M., Christner, B.C., Dore, J.E., Michaud, A.B., Mikucki, J.A., Purcell, A.M., Skidmore, M.L., Priscu, J.C., 2016. Physiological ecology of microorganisms in Subglacial Lake Whillans. Front. Microbiol. 7.

Vick-Majors, T.J., Michaud, A.B., Skidmore, M.L., Turetta, C., Barbante, C., Christner, B.C., Christianson, K., Mitchell, A.C., Achberger, A.M., Mikucki, J.A., Priscu, J.C., 2020a. Biogeochemical characterization of freshwater ecosystems beneath the West Antarctic Ice Sheet and connectivity to the marine coastal environment. Glob. Biogeochem. Cycles 34 (3). https://doi.org/10.1029/2019GB006446.

Vick-Majors, T., Achberger, A., Michaud, A., Priscu, J., 2020b. Metabolic and taxonomic diversity in Antarctic subglacial environments. In: Di Prisco, G., Edwards, H., Elster, J., Huiskes, A. (Eds.), Life in Extreme Environments: Insights in Biological Capability (Ecological Reviews, pp. 279-296). Cambridge University Press, Cambridge. https://doi.org/10.1017/9781108683319.016.

Wedyan, M.A., Preston, M.R., 2008. The coupling of surface seawater organic nitrogen and the marine aerosol as inferred from enantiomer-specific amino acid analysis. Atmos. Environ. 42, 8698–8705.

Wingham, D.J., Siegert, M.J., Shepherd, A., Muir, A.S., 2006. Rapid discharge connects Antarctic subglacial lakes. Nature 440, 1033–1036.

Wright, A., Siegert, M., 2012. A fourth inventory of Antarctic subglacial lakes. Antarct. Sci. 24, 659–664.

Zangrando, R., Barbaro, E., Zennaro, P., Rossi, S., Kehrwald, N.M., Gabrieli, J., Barbante, C., Gambaro, A., 2013. Molecular markers of biomass burning in Arctic aerosols. Environ. Sci. Technol. 47, 8565–8574.